

1 **Knickpoints and Fixpoints: The Evolution of Fluvial Morphology** 2 **under the Combined Effect of Fault Uplift and Dam Obstruction on a** 3 **Soft Bedrock River**

4 Hung-En Chen¹, Yen-Yu Chiu¹, Chih-Yuan Cheng¹ and Su-Chin Chen^{1,2}

5 ¹ Department of Soil and Water Conservation, National Chung Hsing University, Taichung 40227, Taiwan

6 ² Innovation and Development Center of Sustainable Agriculture, National Chung Hsing University, Taichung 40227, Taiwan

7 *Correspondence to:* Su-Chin Chen (scchen@nchu.edu.tw)

8 **Abstract.** Rapid changes in river geomorphology can occur after being disturbed by external factors like earthquakes or large
9 dam obstructions. Studies documenting the evolution of river morphology under such conditions have advanced our
10 understanding of fluvial geomorphology. The Dajia River in Taiwan presents a unique example of the combined effects of a
11 coseismic fault (the 1999 Mw 7.6 Chi-Chi earthquake) and a dam. As a result of the steep terrain and abundant precipitation,
12 rivers in Taiwan have exhibited characteristic post-disturbance evolution over 20 years. This study also considers two other
13 comparative rivers with similar congenital conditions: the Daan River was affected by a thrust fault Chi-Chi earthquake, too;
14 the Zhuoshui River was influenced by dam construction finished in 2001. The survey data and knickpoint migration model
15 were used to analyze the evolution of the three rivers and propose hypothesis models. Results showed that the mobile
16 knickpoint migrated upstream under the influence of flow, while the dam acted as a fixpoint, leading to an increased elevation
17 gap and downstream channel incision. Thereby, the Dajia River narrowing and incision began at both ends and progressively
18 spread to the whole reach under the combined effects.

19 **KEYWORDS:** dam obstruction; fixpoint; coseismic uplift; knickpoint; soft bedrock incision; river evolution

20 1. Introduction

21 Natural tectonic movements and artificial structures are the main factors that disturb river equilibrium. These external
22 influences often interact complexly; therefore, distinguishing between anthropogenic and natural drivers of landscape
23 evolution is difficult. In addition, changes in these external conditions, in turn drive adjustments in the riverbed, generating
24 new landscape patterns. River morphological development generally reflects the geology and flow stress conditions (Lyell,
25 1830). When a significant external impact occurs, a knickpoint (a localized discontinuity in the longitudinal profile of the
26 riverbed) often forms (Holland, 1976). Knickpoints can range in scale from a single waterfall to a zone of several kilometers
27 (Crosby and Whipple, 2006) and may result from natural factors such as extreme weather, sea-level fall, and earthquake-
28 induced surface rupture (Seidl and Dietrich, 1992; Whipple, 2004, Bishop et al., 2005; Heijnen et al., 2020).

29 The active fault causes a prominent knickpoint in stream, known as tectonic uplift, leading to a local increase in channel
30 steepness (Hayakawa et al., 2009; Huang et al., 2013; Cook et al., 2013). The sudden elevation change in the riverbed divides
31 the river profile into two reaches with differing slopes, altering the base level of fluvial erosion. The increasing flow stress
32 erodes the knickpoints, causing it to migrate upstream-ward over time. A long duration is required for the fluvial response to
33 adapt to localized surface uplift or depositional blockage by knickpoint retreat and migration upstream with time, cutting a
34 narrow channel and even forming a canyon. The migration process and speed are highly variable and depend on the tectonic
35 setting and physical nature of the riverbed (Whipple et al., 2004). The emergence and migration of knickpoints caused by
36 disturbance from external conditions was studied extensively (Whipple, 2001; Whipple and Trucker, 2002; Crosby and
37 Whipple, 2006; Clark, 2014; Ahmed et al., 2018).

38 Anthropogenic factors, such as reservoir construction, which is one of the most common ways humans interfere with river
39 hydrology and sedimentation (Magilligan and Nislow, 2005; Petts and Gurnell, 2005; Graf, 2006; Nelson et al., 2013; Liro,
40 2017, 2019; Zhou et al., 2018). Dam as a fixpoint in the river influences two critical components of river geomorphology: the
41 sediment transport capacity of the flow and the oncoming sediment load (Williams and Wolman, 1984). If the sediment
42 transport capacity exceeds the oncoming sediment load, the amount of sediment may be insufficient to maintain the riverbed
43 level, and erosion may occur. Conversely, if the sediment load exceeds the sediment transport capacity, deposition on the
44 riverbed would be expected to occur. The self-adjustment mechanisms of river channels responding to insufficient or excess
45 sediment (Brandt, 2000) results in the change in cross-section geometry, bed material size, river pattern (Leopold and Wolman
46 1957), and slope. Previous studies on the evolution of areas downstream of dams have primarily analyzed changes in

47 downstream sandbars over large spatial scales (Horn et al., 2012; Słowik et al., 2018; Kong et al., 2020) or the ecology of the
48 lower reaches in front of dams (Kingsford, 2000; Braatne et al., 2008; Shafroth et al., 2016). Few studies of exposed bedrock
49 have been based on long-term observations (Inbar, 1990). In most cases, a dam effectively traps the sediment supply from the
50 watershed. If sediment transfer to the downstream reaches of the dam is reduced, the armor layers of the riverbed are lost,
51 which may cause an incision of the fluvial channel (Surian and Rindai, 2003). This incision subsequently narrows the river
52 cross-sections and lowers the thalweg level.

53 Decades or hundreds of years are generally required for a riverbed to reach a new equilibrium after disturbance by external
54 conditions, so it is difficult to understand such changes based on short-period observational data (Howard et al., 1994; Tomkin
55 et al., 2003). Because of the abundant rainfall brought by typhoons and monsoons, the river terrain in Taiwan can alter
56 dramatically over a short period of time. Moreover, dams in Taiwan are built primarily in steep reaches, enhancing the rapid,
57 remarkable morphological evolution of the downstream reaches. The reservoirs of dams constructed on the rivers become
58 silted up, resulting in a lack of sediment downstream in the meantime, which causes loss of armor layers, exposure of soft rock,
59 and severe erosion. Another factor influencing the distinctive characteristics of Taiwanese rivers is the geological location;
60 Taiwan is located in a plate junction zone that experiences frequent earthquakes such as the Chi-Chi Earthquake of 1999 (Lin
61 et al., 2001; Ota et al., 2005), which caused the offset of Chelungpu thrust fault in central Taiwan. The surface rupture and
62 uplift induced the formation of knickpoints and river gorges. Twenty years later, the undercutting trend of the active channel
63 below dams and the migration of post-earthquake knickpoints have caused the rivers to evolve into their present forms. This
64 rapid evolution of river morphology over a short time makes Taiwan rivers suitable as case studies. The Dajia River is a unique
65 example, as a dam structure and coseismic uplift impact it simultaneously in a short reach. The current work aims to clarify
66 the river changes caused by the earthquake and a dam, and to propose a hypothesis for the evolution model. To compare the
67 various morphological developments under different external conditions, the Daan, Zhuoshui, and Dajia rivers in central
68 Taiwan are considered in this study.

69 **2. Study area, materials, and methods**

70 The longitudinal changes of the river bed and the accompanying river pattern changes are the objects of observation. A
71 common type of longitudinal profile development for knickpoint retreat is illustrated in Fig. 1a (Gardner 1983; Whipple and
72 Trucker, 1999; Parker and Izumi 2000; Alonso et al. 2002; Bressan et al., 2014). As the base level of erosion fell, the stream
73 encountered an abrupt shift in slope from gentle to steep, which significantly accelerated the flow and subsequently led to

74 stream bed erosion. During this process, apparent upstream degradation and downstream aggradation occurred. The knickpoint
75 migrated upward with time, accompanying by slope replacement. After the river had reached a new equilibrium in a channelized
76 pattern, the slope replacement resulted in a natural profile. During the adjustment, the incision trend gradually slowed, and
77 sedimentation may commence downstream (dashed line in Fig. 1a). The profile evolved from a concave curve to a graded
78 profile (Chamberlin and Salisbury, 1904). The well-known result of dam construction is the progressive loss of the armor layer
79 in the neighboring downstream river (Fig. 1b). The scouring baseline extended downstream-ward from the dam (Olsen, 1999;
80 Choi et al., 2005; Słowik et al., 2018). Because of the fixpoint, the local slope at the dam toe became steeper progressively,
81 and the dam caused the downstream river profile to be gentle and sediment transport to decrease.

82 However, significant changes in the longitudinal profile must also be accompanied by variations in river patterns, which
83 have yet to receive much attention. Furthermore, the interaction between fault scarps and dam obstructions within a river reach
84 is rarely observed and studied. To address these gaps, we collected historical data (incl. multiyear satellite images, orthographic
85 images, cross-sectional and longitudinal profiles.) for three rivers in Taiwan (Daan, Zhuoshui, and Dajia), each representing
86 the individual effects of faults and dams, as well as their combined effects.

87 2.1 Study area

88 Taiwan's climate is strongly affected by the western Pacific tropical cyclone. There are approximately three to four
89 typhoons and heavy rain events yearly, and the average annual precipitation is about 2500 mm. The heavy rains during the
90 monsoons and typhoons cause dramatic changes to riverbeds over short periods of time. In addition, because Taiwan is located
91 at the compressive tectonic boundary between the Eurasian and Philippine Sea plates, the collision of the two continental plates
92 causes tectonic breakage of the strata. On September 21, 1999, the Chi-Chi earthquake ($M_w = 7.6$) resulted in uneven uplift in
93 the island. Three central Taiwan rivers illustrate dams or faults' effects (Figure 2): The Daan River has been affected by vertical
94 fault scarps, the Dajia River by both fault scarps and a dam, and the Zhuoshui River by dam obstruction. These three important
95 rivers have very similar characteristics: their east-to-west flow direction; their range of elevation from sea level to ~3000 m;
96 their steep river slopes (the average slope of each river 1.5% – 2.4%, Kuo et al.(2021)); and the presence of soft rock in the
97 mid-stream (as shown in the pink region in Fig. 2). The locations of the three rivers and the Chelungpu thrust fault are marked
98 in Fig. 2. The southern termination of the fault crosses the Zhoushui River trending north–south; the northern termination near
99 the Dajia and the Daan rivers shows a complex deformation pattern trending NE–SW to E–W (Lee et al., 2002), composed of
100 several parallel thrust faults. In the three studied reaches, the Pleistocene sedimentary rocks are mainly composed of soft rocks

101 consisting of sandstone, siltstone, shale, and mudstone. Soft rocks have intermediate strength between soils and hard rocks
102 with possessing unconfined compressive strengths ranging from 0.5 to 25.0 MPa (Lai et al., 2011). These rocks are generally
103 poorly lithified and weakened by a high water content; therefore, their resistance to water erosion is poor. The riverbed rock is
104 readily incised by flooding flow when the upper armoring protective layer was lost (Huang et al., 2014).

105 The Chi-Chi earthquake produced a surface rupture 80 km long. Several fracture planes at the north end of the fault
106 caused uneven uplift in the region (Lee et al., 2002). One of the ruptures passed through the right bank of the Shigang Dam
107 (constructed in 1977) on the Dajia River, causing serious damage to the dam structure. The maximum vertical displacement of
108 the surface rupture was 9 m, increasing the drop height of the bed level between the face and the back of the dam markedly.
109 The dam reconstruction was finished in 2000. The repaired Shigang Dam was intended to store 2.4×10^6 m³ of water after the
110 Chi-Chi earthquake; however, owing to deposition in the reservoir, only $\sim 1.4 \times 10^6$ m³ of water can now be retained. After the
111 earthquake and the reconstruction, the fluvial morphology has been changed rapidly. The original armor layers on the riverbed
112 in front of the Shigang Dam were lost rapidly, and the soft bedrock was exposed. The two rupture surfaces at the north end of
113 the Chelungpu Fault uplifted a 1 km reach of bed in the Daan River, with a maximum vertical uplift of 10 m.

114 Although the southern end of the Chelungpu Fault passes downstream of the Jiji Dam (Zhuoshui River), the fault uplifted
115 the bed level by ~ 2 m, less than the uplifts in the Daan and Dajia rivers. The Jiji Dam was built in 2001 (after the 1999 Chi-
116 Chi earthquake), is situated on the narrowest part of the Zhuoshui River, and has a maximum designed storage capacity of 10
117 $\times 10^6$ m³. Due to the large sediment yield in the Zhuoshui River watershed, the present-day adequate water storage capacity is
118 only $\sim 4 \times 10^6$ m³. The Jiji Dam downstream is known for its soft bedrock canyon features, formed by dam-obstructed water
119 scouring.

120 **2.2 Materials**

121 Analysis of the effects of faults and dams, alteration of river patterns, changes in thalweg levels, and variations in river
122 cross-sections are crucial to revealing the process of river evolution. SPOT-5 and SPOT-6 satellite images (2 m in
123 resolutions) and orthographic images (25 – 50 m in resolutions) obtained by the Center for Space and Remote Sensing
124 Research, National Central University (CSRSR/NCU) and the Aerial Survey Office (AFASI) of Taiwan were used to
125 assess changes in river patterns. Multiyear cross-sectional and longitudinal profiles were established from historical
126 surveys by the Water Resources Agency (WRA). The survey was conducted using Total Station, GPS, and depth sounder.
127 The interval of survey points should be 5–10 m, and the elevation error must not exceed cm. Additional analyses of

knickpoint retreat and variations in river elevation and width were carried out. The locations of knickpoints were determined by identifying abrupt terrain changes and the positions of splash in the images. In order to analyze the variation of channel width (W), depth (D), and aspect ratio (W/D), we calculated the bank-full discharge width and depth, which represents the maximum flow that can occur in a river before water starts overflowing and spreading out onto the floodplain. We identified the river banks and extracted channel widths from orthographic images. The banks were defined as the boundaries between the main channel and the adjacent floodplain.

2.3 Mathematical model

The application of the mathematical model provides an abstract description of a concrete system using physical concepts and mathematical language. A one-dimensional Exner equation (Exner, 1925) is used to describe the advective and diffusive knickpoint migration (Bressan et al., 2014):

$$\frac{\partial z}{\partial t} + \frac{1}{(1-p_s)} \frac{\partial q_s}{\partial x} = 0 \quad (1a)$$

where z is the bed elevation along the thalweg, p_s is the porosity of bed sediment, t is the time, x is the distance, and q_s is the sediment discharge per unit width that is estimated by the product of the surface height change η , and the knickpoint migration rate dx/dt is expressed as equation 1b.

$$q_s = -\eta \frac{dx}{dt} \quad (1b)$$

The migration rate as a sediment separation per unit area homogeneously distributed over the eroding surface is expressed as equation (1c).

$$\frac{dx}{dt} = k_d [\tau(x) - \tau_c] \quad (1c)$$

where k_d is the erodibility, τ is the bed shear stress, and τ_c is the critical shear stress of the bed material. The condition of an obvious knickpoint face, τ should be estimated using a formula that considers knickpoint as a submerged obstacle (equation (1d)) (Engelund, 1970).

$$\tau(x) = M\tau_0 \left[1 + A \frac{(z-z_0)}{H_0} + B \frac{\partial z}{\partial x} \right] \quad (1d)$$

The factors M , A , and B in equation (1d) are parameters related to localized phenomena. τ_0 , z_0 , and H_0 are the shear stress, bed elevation and the water depth upstream of the knickpoint. The term $B \frac{\partial z}{\partial x}$ represents the change in shear stress due to the local slope. The shear stress in the channel section upstream of the knickpoint crest ($\tau_0 = \gamma H_0 S_0$, where γ is the specific weight of water changes across the knickpoint due to the abrupt change in bed topography (equation (1d)). Substituting equations (1b)–(1d) into equation (1a), equations (2a)–(2c) were obtained in below:

$$155 \quad \frac{\partial z}{\partial t} - C \frac{\partial z}{\partial x} - D \frac{\partial^2 z}{\partial x^2} = 0 \quad (2a)$$

$$156 \quad C = \left(\frac{\eta^k_{dY}}{1-p_s} \right) S_0 MA \quad (2b)$$

$$157 \quad D = \left(\frac{\eta^k_{dY}}{1-p_s} \right) S_0 H_0 MB \quad (2c)$$

158 where the coefficients of the first- and second-order spatial derivatives, C and D , are known as the advection and diffusion
 159 coefficients, respectively. It can be concluded that the key controls of the knickpoint retreat are the channel slope, the erodibility
 160 of the bed of the river reach, the knickpoint face height, and the upstream water depth. Therefore, the present equation is a
 161 physical-based model that can be solved with the second-order accurate implicit finite difference scheme which was
 162 implemented in MATLAB. However, it is essential to recognize that the numerical model is conceptual and involves several
 163 assumptions, such as not considering variations in the horizontal 2D plane of the terrain and assuming homogeneous
 164 parameters within the simulation area, among others. The numerical model cannot fully capture the actual scenario's detailed
 165 morphology and environmental conditions; it serves as a conceptual model based on physical mechanisms, providing trends
 166 rather than precise representations.

167 3. RESULTS

168 3.1 Fault effect on Daan River canyon

169 The scarps across the Daan River that were uplifted by the Chi-Chi earthquake caused a dramatic change in the topography,
 170 disturbing the dynamic equilibrium of the fluvial system. Cook et al. (2013) proposed that the knickpoint propagated rapidly
 171 after 2004 and pointed out that the tool effect caused pronounced fluvial incision of the bedrock after the disappearance of
 172 bedload. Knickpoint propagation was influenced by the antiformal geological structure of the area, the presence and orientation
 173 of interbedded strong and weak lithologies, and the proportion of discharge entering the main channel. Huang et al. (2013)
 174 also proposed that the knickpoint retreat rate can be affected by several factors, including discharge, rock properties, geological
 175 structures, and bedrock orientation. The channel development of the studied reach and the behavior of knickpoint retreat were
 176 assessed by analyzing multiyear data on the form and cross-section of the river.

177 Successive orthographic images of the studied reach of the Daan River from 2000 to 2017 and the corresponding flow
 178 paths are illustrated in Fig. 3. River cross-sections constructed from precise survey data are provided in Fig. 4. Chronological
 179 longitudinal profiles of the river reach are shown in Fig. 5. Longitudinal profile data from Cook et al. (2013) were included to
 180 make information more complete. The effect of the earthquake on the surface elevation is clearly visible in Fig. 5. In addition

181 to the survey data, the advective and diffusive knickpoint migration model (equation 2) was solved to mathematize the
182 knickpoint retreat progress after the Chi-Chi earthquake. The initial condition and boundaries condition are needed to solve
183 the equation. The initial condition is the longitudinal profile in 1999, while the boundary conditions are the real bed changes
184 in upstream and downstream boundaries. The C and D are physical parameters and were calibrated by the survey data. In
185 equation 2, C represents the moving speed, and D represents the diffusion constant. These two coefficients reflect the rate of
186 bed erosion, which is physically composed mainly of bed shear stress (equations 2b and 2c). Due to the actual bed erosion
187 rates varying with time, the parameters were adjusted to match the real changes. Before 2004, C was 22.0 m/yr, and D was
188 $10.0 \text{ m}^2/\text{yr}$; after 2004, C was 91.5 m/yr, and D was $18.5 \text{ m}^2/\text{yr}$, and the simulation was continued until 2011 when the
189 knickpoint disappear. The result of the modeling is shown at the top left corner in Fig. 5. The knickpoint progressively retreats,
190 accompanying by slope replacement. The variation trend of the simulation and survey data is generally consistent, and the speed
191 (C) has a larger value in 2004 – 2011, which is also consistent with the observation.

192 The long-term development of the studied reach of the Daan River in the past 20 years, after the coseismic uplift, can be
193 divided into three periods: downstream erosion and slow knickpoint migration (earthquake to 2004); sudden migration of the
194 knickpoint (2004 – 2011); and gorge widening and eradication (2011 – present).

195 **3.1.1 Downstream erosion and slow knickpoint migration (earthquake to 2004)**

196 After the Chi-Chi earthquake, coseismic ground deformation created a pop-up obstruction across the river, forming a
197 barrier lake behind the rupture scarp. The obstacle blocked the river flow and trapped the sediment, causing the river bed
198 downstream of the rupture scarp completely lose the armor layer. When the armor layer was lost, bedrock incision occurred
199 downstream of the uplifted zone, and the knickpoint retreat appeared. On the other hand, no significant erosion occurred
200 between cross-sections **a** and **b** during that period (Figs 3 and 4). A comparison of the cross-sections for 2000 and 2004 (Fig.
201 4) reveals that most parts of the section **a** even experienced deposition. Slight erosion in some places can be detected in the
202 longitudinal profiles (Fig. 5) between 1999 (after the earthquake) and 2004. Although the seismic uplift produced an obvious
203 knickpoint on the riverbed, that knickpoint migrated only slightly (85 m; Table 1) between 2000 and 2004. The downstream
204 reach of the uplifted zone showed evidence of scour, but no noticeable bedrock incision or canyon landscape had developed
205 yet.

206 **3.1.2 Sudden migration of knickpoint (2004–2011)**

207 The orthographic image for 2007 (Fig. 3) clearly shows that the armor layer had been removed, the bedrock had been

208 exposed, and the deep incision had formed a narrow channel. The knickpoint retreated upstream-ward by approximately 422
209 m between 2004 and 2007, accompanied by continued scouring downstream. In the uplifted reach, under the stress of the
210 concentrated flow in the newly formed channel, the tool effect resulted in a deepened incision of the rock bed, and a canyon
211 landform gradually developed. In the 2007 cross-section data for section **a**, a canyon close to the left bank can be observed,
212 which persisted until 2011. A rapid incision rate (5.6 m/yr) occurred in section **a**, which also experienced a narrowing rate of
213 about 105.5 m/yr. Bed incision and narrowing of the main channel occurred in section **b** simultaneously, with a narrowing rate
214 of approximately 89.9 m/yr and an incision rate of about 2.1 m/yr. Between 2007 and 2011, the knickpoint retreated upstream
215 by about 412 m; the incision at section **a** was lessened, but section **b** experienced a notable incision into the rock bed
216 accompanied by knickpoint retreat. Because an obvious gorge channel had appeared in the uplifted zone, sediment from
217 upstream was transported downstream, and downstream scouring transformed gradually into sedimentation; therefore, the
218 convex longitudinal profile was gradually erased.

219 **3.1.3 Gorge widening and eradication (2011 to the present)**

220 After 2011, the knickpoint became insignificant in the longitudinal profile, so the thalweg scouring trend slowed. The
221 morphology development is dominated by lateral erosion instead of vertical incision. The narrow, deep canyon evolved into a
222 U-shaped canyon with a wide bottom. River pattern migration from upstream caused the canyon-type channel to commence
223 transforming into a braided channel. The main channel of section **a** experienced deposition as a result of the sediment supply
224 being adequate (Fig. 5). Cook et al. (2014) proposed a mechanism of gorge eradication, called *downstream sweep erosion*,
225 which rapidly transformed the gorge into a beveled floodplain through the downstream propagation of a wide erosion front
226 located where the broad upstream channel abruptly became a narrow gorge. The sweep boundary is clearly visible in the
227 orthographic images for 2011 and 2017 (Fig. 3). Additional large floods are expected to cause a marked widening of the channel
228 instead of deepening (Huang et al., 2013). It has been estimated that removal of the gorge erosion will take 50 years (Cook et
229 al., 2014).

230 Significant incision of the channel is common after a riverbed has been uplifted suddenly by tectonic movement and the
231 bed slope changes dramatically (Merritts et al., 1989). This was the case for the Daan River after the Chi-Chi earthquake. After
232 the coseismic uplift, the base level of erosion downstream reduced, so erosion increased. The river width became notably
233 narrower and deeper. Upward movement of the knickpoint caused the river channel in the uplifted section to narrow rapidly.
234 The concentrated flow caused a rapid incision of a weak geological layer in the riverbed, so the channel width decreased

235 sharply. Therefore, the uplifted section formed a canyon landform. As the slope at the knickpoint gradually recovered, the
236 incision slowed and sediment transport down the recovered river resulted in sediment deposition in the downstream channel.
237 The river also gradually developed lateral erosion upstream, and the river channel tended to widen. The channelization is
238 expected to have been swept because the sweep boundary migrated progressively downward.

239 3.2 Jiji Dam effect on Zhoushui River

240 Construction of the Jiji Dam on the Zhoushui River began in 1996 and operated in 2001. Orthographic images, flow paths
241 of the studied reach, and the locations of cross-sections **c**, **d**, and **e** below the Jiji Dam for 1998 to 2018 are provided in Fig. 6.
242 Chronological survey data of cross-sections **c**, **d**, and **e** are provided in Fig. 7. Chronological longitudinal profiles of the studied
243 reach are illustrated in Fig. 8. The river is located at the southern termination of the Chelungpu Fault (Fig. 1), where the
244 elevation gap caused by the earthquake is relatively small. In 1998, the Zhoushui River was a broad braided river, with many
245 sandbars downstream of the dam (Fig. 6). In 2003, two years after dam operation had commenced, the riverbed armor layer
246 had been lost and the exposed soft bedrock was clearly visible within 700 m of the toe of the dam, because of a lack of sediment.
247 The bedrock's incision deepened due to the tool effect, and the flow path concentrated gradually in front of the dam. From
248 2003 to 2007, the effect zone gradually expanded, and exposed bedrock extended to ~3.2 km downstream from the dam.
249 Between 2007 and 2018, the channelization and the zone with exposed bedrock expanded continuously to 6.5 km downstream
250 of the dam. Due to the channelization, the river cross-section became narrow and deep.

251 The transformation of the river and the rates of lateral and vertical change are clearly visible in the river cross-sections
252 (Fig. 7). There was no apparent erosion of section **c** in 2008, but the sections closer to the dam (**d** and **e**) exhibited obvious
253 incision (Fig. 7). After the loss of the riverbed armor layer, the flow cut down into weak bedrock. The deep main channels'
254 development is clearly visible in sections **d** and **e** between 1998 and 2008. During this time, the incision rate of section **e** was
255 around 1.2 m/yr, and the narrowing rate was around 25 m/yr. During 2008 – 2012, engineering measures were installed:
256 between section **d** and section **e**, groundsills, spur dikes and tetrapod were added to the river channel to prevent erosion, and
257 the riverbed level rose slightly at section **e**. However, the channel width of section **c** was markedly narrower, with a narrowing
258 rate of roughly 65 m/yr. Between 2008 and 2015, the incision rates of sections **c** and **d** were roughly 1.4 m/yr. Progressive
259 erosion layer by layer is apparent in the chronological longitudinal profiles (Fig. 8). Incision of the studied reach became
260 increasingly severe: incision commenced at section **e** and subsequently extended downstream to sections **d** and **c**. We infer that
261 headward erosion did not dominate the riverbed because the Chelungpu Fault passed through the river some distance from the

262 dam and caused only 2 m of uplift; on the contrary, dam-induced downward incision of the riverbed caused degradation of the
263 reach. There is an approximately 15 m difference between the bed level of 1998 and that of 2018.

264 3.3 The combined effect of Shigang Dam and Fault on Dajia River

265 The studied reach of the Dajia River, which lies downstream of the Shigang Dam, was affected by both the dam and uplift
266 caused by the Chi-Chi earthquake. The Shigang Dam was broken by uneven uplift of the fault scarp across the dam (9 m on
267 the right side and 3 m on the left), and the downstream section **f** rose by ~ 7 m (see Fig. 2). The earliest knickpoint formed close
268 to section **f** and moving headward with time. During 2000–2005, the knickpoint retreated by ~ 40 m, and another new
269 knickpoint formed between sections **g** and **h** (Fig. 9) under the co-effect of river pattern changes and bed rock differential
270 erosion. The damming effect of the Shigang Dam also caused the armor layer to be removed. The bedrock became exposed
271 shortly after the earthquake; however, section **f** was obviously incised during 2000–2005, whereas incision of section **g** did not
272 occur until 2005–2008 (Fig. 10). Between 2000 and 2005, engineering measures were installed on several occasions to mitigate
273 the obvious erosion. The river pattern between section **g** and the dam was a braided river during the period.

274 The incision rate of section **g** was ~ 1.1 m/yr during 2005–2008, and the narrowing rate was ~ 47.7 m/yr. During the same
275 time interval, the downstream knickpoint (between sections **f** and **g**) disappeared due to river training in 2008. The knickpoint
276 between section **g** and section **h** retreated rapidly toward the dam (Figs 9, 11). During 2005–2008 and 2008–2017, the
277 knickpoint moved upstream by approximately 186 and 219 m, respectively. This retreat of the knickpoint implies that river
278 channel scouring did not stop. Because the riverbed strata trend northeast–southwest, flow scouring preferentially deepened
279 the left part of the rock bed, which moved the channel closer to the left bank. After 2008, the flow channel extended closer to
280 the toe of the dam. Due to the severe incision, the government started surveying section **h** after 2010 (Fig. 10). Significant
281 bedrock incision was recorded, with an incision rate of ~ 1.4 m/yr at section **h** during 2010–2017. In 2008, it can be observed
282 that the knickpoint existed in the reach between sections **g** and **h**; therefore the slope of the channel is still discontinuous. The
283 2017 photograph shows a single, meandering channel that starts from the dam and runs through sections **h** and **g**, eventually
284 reaching section **f**, where the knickpoint had initially formed (Fig. 10). Overall, the area downstream of the Shigang Dam
285 displayed headward erosion of the knickpoint and incision of the rock bed in front of the dam.

286 In the Dajia River, the advection and diffusion equation (equation 2) was also used to represent the variation mode of
287 knickpoint and bed elevation. The initial condition is the longitudinal profile in 2000. The coefficients C and D were influenced
288 by bed shear stress. Due to the rapid increase in actual bed erosion rate after 2005, the parameters were adjusted to match the

289 actual changes. Before 2005, C was 7.5 m/yr, and D was 1.825 m²/yr; after 2005, C was 36.5 m/yr, and D was 9.125 m²/yr, and
290 the simulation was continued until 2017. The downstream boundary adopts the real bed change, while the upstream boundary
291 condition is fixed, considering the dam is a fixed point. The bed is progressively scoured in the nearby downstream of the dam,
292 and the knickpoint retreats and gradually fades away. The variation trend of the simulation and survey is generally consistent,
293 excluding the fact that intensive engineering works have been conducted in front of the dam to stabilize the bed.

294 4. Discussion

295 Data on the changes in the riverbed, river width, and migration distance of the knickpoint for all three studied reaches are
296 provided in Table 1. Also, in Fig. 12(a), We use “T” symbols to represent the channel width (W) and depth (D) of the cross-
297 sections in three study reaches. The aspect ratio (W/D) is labeled above every “T.” After the Chi-Chi earthquake, the channel
298 geometry was not disturbed immediately. The aspect ratio of the Daan River exhibited only slight changes. Consequently, the
299 aspect ratio significantly decreased with time from the downstream section; subsequently, the aspect ratio recovered a little
300 after 2011. The deepening of the upstream was slower than that downstream, but the later recovery was more obvious in the
301 upstream area. The aspect ratio of the Zhuoshui River dramatically declined in the upstream part after construction of the Jiji
302 Dam; this change extended gradually to the downstream section with time. In the Dajia River, owing to the combined effects
303 of the upstream dam and the earthquake, channelization of the river started at both ends of the reach and then met in the middle.
304 The examples of these three rivers allow us to deduce the evolution of knickpoint retreat and transformation of the river pattern
305 under the influence of dams and/or uplift.

306 The river pattern of knickpoint retreat is illustrated in Fig. 12(b), and it was also observed in the Daan River. During the
307 knickpoint retreat, the tool effect caused the river to narrow dramatically. However, after the river had reached a new
308 equilibrium in a channelized pattern, the slope replacement resulted in a natural profile. The incision trend gradually slowed
309 during the adjustment, and sedimentation may commence downstream (dashed line in Fig. 12(b)). The profile evolved from a
310 concave curve to a graded profile (Chamberlin and Salisbury, 1904). In the case of the Daan River, the topography of the
311 upstream gorge was gradually swept away, and the river pattern may be slowly restored to the original braided plain.

312 Before construction of the Jiji Dam, the studied reach of the Zhoushui River was a broad braided river. The river armor
313 layer was lost due to sediment trapping by the dam. Under the influence of the tool effect, the flow path in front of the dam
314 gradually narrowed (Fig. 12(c)). The scouring boundary extended downstream-ward from the dam. Because of the immovable
315 knickpoint, the local slope at the dam toe became steeper, and the dam (acting as a non-erasable knickpoint) caused the river

316 profile and sediment transport to remain non-equilibrium.

317 The reach downstream of the Shigang Dam on the Dajia River was simultaneously affected by coseismic uplift and the
318 incision of a deep path in the soft rock in front of the dam. The knickpoint caused by fault uplift retreated upward with time.
319 Although the uplift of the Dajia River was similar to that of the Daan River, the Shigang Dam (fixpoint) restricted knickpoint
320 retreatment in the Dajia River, and led to scouring downward from the dam site. Therefore, we saw the river narrowing at the
321 two ends of the affected reach, then progressively extending to the middle, as shown in Fig. 12(d). The knickpoint caused by
322 the earthquake was gradually removed, but the effect of the dam remains. Therefore, the start of recovery to a braided river
323 cannot happen in the Dajia River.

324 In Fig 13, the discharge data of outflow from Shigang Dam (Dajia River) and Jiji Dam (Zhuoshui River), and the flow
325 data of the Daan River from July 2005 to December 2019. The cumulative flow results show that the increasing trends of the
326 discharge in the Dajia and Zhuoshui Rivers are consistent. Both dams serve the purpose of controlling water levels for water
327 supply and irrigation. The direct discharge is influenced by the variations in dry and rainy seasons, resulting in intermittent
328 changes in the discharge. In contrast, the flow in the Daan River shows continuously and stable increasing. We observed a
329 positive correlation between the knickpoints retreat distances and the cumulative discharge in the Dajia River and also in Daan
330 River. However, the correlation between flow and retreat distance does not exist when comparing different rivers. Additionally,
331 A relationship between discharge and the changes in channel widening or the incision depth cannot be found.

332 Overall, there are apparent differences in the morphological changes to rivers caused by natural and human factors. A
333 knickpoint formed by fault-induced riverbed uplift is a moving point: as the knickpoint moves, the riverbed evolves gradually
334 from an unstable state to an equilibrium. In contrast, a dam can be regarded as a fixpoint on the river. The flow from the
335 spillway outlet hits the riverbed continuously, resulting in a decline of the erosion base level; therefore, downward erosion
336 commences from the toe of the dam. For the case under the combined effect of fault uplift and dam obstruction, we inferred a
337 schematic diagram of longitudinal profile development for the combined effects as shown in Fig. 14. In Fig 14, the uplift
338 creates knickpoints that gradually retreat upstream. Meanwhile, Starting from the dam toe, the continuous deepening. When
339 these two phenomena meet, changes resulting from natural tectonic movements of a riverbed may achieve equilibrium with
340 time, whereas imbalance caused by anthropogenic structures may be enhanced with time.

341 5. Conclusions

342 The Daan River, Zhoushui River, and Dajia River in central Taiwan exhibited changes in river morphology after

343 disturbance by earthquake uplift and dam obstruction during the past 20 years. The Daan River was affected by a thrust fault;
344 the Zhuoshui River was influenced by dam obstruction; and the Dajia River was both fault- and dam-influenced. In the Daan
345 River, the greater slope accelerated the flow velocity and drove knickpoint retreat after removal of the armor layer, resulting
346 in the progress of slope replacement. However, the incision faded with time, sediment deposition commenced, and the river
347 showed potential for recovery to braided river pattern. Because of sediment trapping by the Jiji Dam, the Zhoushui River has
348 transformed from braided to gorge. The channelization started from the dam and expanded downward, and the incision progress
349 caused the local slope at the toe to become steeper. Because the dam acts as an immovable knickpoint, the river's sediment
350 equilibrium could not be re-established. The Shigang Dam on the Dajia River also caused a downward incision. The incision
351 from the toe of the dam subsequently connected with the knickpoint retreat caused by headward erosion from downstream,
352 forming a single, meandering channel at the front of the dam.

353 Knickpoints resulting from fault-induced riverbed uplift are moving points: as the knickpoint moves, the riverbed
354 evolves gradually from an unstable state to an equilibrium state. In contrast, a dam, as a fixpoint on the river, causes continuous
355 degradation. When both effects exist on a reach, the impact of the knickpoint gradually fades away, but the results of the dam
356 on the river persist.

357 **Author contribution**

358 The authors made the following contributions: HEC was involved in methods development, modeling, data analysis,
359 discussion, and paper preparation. YYC participated in data analysis, discussion, and paper preparation. CYC conducted the
360 field survey, collected and analyzed data. SCC contributed to the hypothesis, concept, research design, conclusions, and
361 paper preparation.

362 **Competing interests**

363 The authors declare that they have no conflict of interest.

364 **Acknowledgements**

365 The Ministry of Science and Technology, Taiwan, partially supports this research under grant No. 111-2625-M-005-001.
366 The authors would like to thank AFASI, MOST, and CSRSR/NCU for supplying satellite imagery data and WRA for supplying
367 river measurement data.

368 **References**

- 369 Ahmed, M. F., Rogers, J. D., and Ismail, E. H.: Knickpoints along the upper Indus River, Pakistan: an exploratory survey of
370 geomorphic processes, *Swiss Journal of Geosciences*, 111, 191-204, <https://doi.org/10.1007/s00015-017-0290-3>, 2018.
- 371 Alonso, C. V., Bennett, S. J., and Stein, O. R.: Predicting head cut erosion and migration in concentrated flows typical of
372 upland areas, *Water Resources Research*, 38, 39-31-39-15, <https://doi.org/10.1029/2001wr001173>, 2002.
- 373 Bishop, P., Hoey, T. B., Jansen, J. D., and Artza, I. L.: Knickpoint recession rate and catchment area: the case of uplifted
374 rivers in Eastern Scotland, *Earth Surface Processes and Landforms*, 30, 767-778, <https://doi.org/10.1002/esp.1191>, 2005.
- 375 Braatne, J. H., Rood, S. B., Goater, L. A., and Blair, C. L.: Analyzing the impacts of dams on riparian ecosystems: a review
376 of research strategies and their relevance to the Snake River through Hells Canyon, *Environmental Management*, 41, 267-
377 281, <https://doi.org/10.1007/s00267-007-9048-4>, 2008.
- 378 Brandt, S. A.: Classification of geomorphological effects downstream of dams, *Catena*, 40, 375-401,
379 [https://doi.org/10.1016/S0341-8162\(00\)00093-X](https://doi.org/10.1016/S0341-8162(00)00093-X), 2000.
- 380 Bressan, F., Papanicolaou, A. N., and Abban, B.: A model for knickpoint migration in first- and second-order streams,
381 *Geophysical Research Letters*, 41, 4987-4996, <https://doi.org/10.1002/2014GL060823>, 2014.
- 382 Chamberlin, T. C., and Salisbury, R. D.: *Geology: Geologic processes and their results*, H. Holt, 1904.
- 383 Choi, S. U., Yoon, B., and Woo, H.: Effects of dam-induced flow regime change on downstream river morphology and
384 vegetation cover in the Hwang River, Korea, *River Research and Applications*, 21, 315-325, <https://doi.org/10.1002/tra.849>,
385 2005.
- 386 Clark, M. K., Maheo, G., Saleeby, J., and Farley, K. A.: The non-equilibrium landscape of the southern Sierra Nevada ,
387 California, 5173, [https://doi.org/10.1130/1052-5173\(2005\)15](https://doi.org/10.1130/1052-5173(2005)15), 2014.
- 388 Cook, K. L., Turowski, J. M., and Hovius, N.: A demonstration of the importance of bedload transport for fluvial bedrock
389 erosion and knickpoint propagation, *Earth Surface Processes and Landforms*, 38, 683-695, <https://doi.org/10.1002/esp.3313>,
390 2013.
- 391 Cook, K. L., Turowski, J. M., and Hovius, N.: River gorge eradication by downstream sweep erosion, *Nature Geoscience*, 7,
392 682-686, <https://doi.org/10.1038/ngeo2224>, 2014.
- 393 Crosby, B. T., and Whipple, K. X.: Knickpoint initiation and distribution within fluvial networks: 236 waterfalls in the
394 Waipaoa River, North Island, New Zealand, *Geomorphology*, 82, 16-38, <https://doi.org/10.1016/j.geomorph.2005.08.023>,
395 2006.
- 396 Gardner, T. W.: Experimental study of knickpoint and longitudinal profile evolution in cohesive, homogeneous material,
397 *Geological Society of America Bulletin*, 94, 664-672, 1983.
- 398 Graf, W. L.: Downstream hydrologic and geomorphic effects of large dams on American rivers, *Geomorphology*, 79, 336-
399 360, <https://doi.org/10.1016/j.geomorph.2006.06.022>, 2006.
- 400 Hayakawa, Y. S., Matsuta, N., and Matsukura, Y.: Rapid recession of fault-scarp waterfalls: Six-year changes following the
401 921 Chi-Chi Earthquake in Taiwan, *Chikei/Transactions, Japanese Geomorphological Union*, 30, 1-13, 2009.
- 402 Heijnen, M. S., Clare, M. A., Cartigny, M. J. B., Talling, P. J., Hage, S., Lintern, D. G., Stacey, C., Parsons, D. R., Simmons,
403 S. M., Chen, Y., Sumner, E. J., Dix, J. K., and Hughes Clarke, J. E.: Rapidly-migrating and internally-generated knickpoints
404 can control submarine channel evolution, *Nature Communications*, 11, 3129-3129, [https://doi.org/10.1038/s41467-020-
405 16861-x](https://doi.org/10.1038/s41467-020-16861-x), 2020.
- 406 Holland, W. N., and Pickup, G.: Flume study of knickpoint development in stratified sediment, *Geological Society of
407 America Bulletin*, 87, 76-82, [https://doi.org/10.1130/0016-7606\(1976\)87<76:FSOKDI>2.0.CO;2](https://doi.org/10.1130/0016-7606(1976)87<76:FSOKDI>2.0.CO;2), 1976.

408 Horn, J. D., Joeckel, R. M., and Fielding, C. R.: Progressive abandonment and planform changes of the central Platte River
409 in Nebraska, central USA, over historical timeframes, *Geomorphology*, 139, 372-383,
410 <https://doi.org/10.1016/j.geomorph.2011.11.003>, 2012.

411 Howard, A. D., Dietrich, W. E., and Seidl, M. A.: Modeling fluvial erosion on regional to continental scales, *Journal of*
412 *Geophysical Research*, 99, <https://doi.org/10.1029/94jb00744>, 1994.

413 Huang, M.-W., Pan, Y.-W., and Liao, J.-J.: A case of rapid rock riverbed incision in a coseismic uplift reach and its
414 implications, *Geomorphology*, 184, 98-110, <https://doi.org/10.1016/j.geomorph.2012.11.022>, 2013.

415 Huang, M. W., Liao, J. J., Pan, Y. W., and Cheng, M. H.: Rapid channelization and incision into soft bedrock induced by
416 human activity - Implications from the Bachang River in Taiwan, *Engineering Geology*, 177, 10-24,
417 <https://doi.org/10.1016/j.enggeo.2014.05.002>, 2014.

418 Inbar, M.: EFFECT OF DAMS ON MOUNTAINOUS BEDROCK RIVERS, *Physical Geography*, 11, 305-319,
419 <https://doi.org/10.1080/02723646.1990.10642409>, 1990.

420 Kingsford, R. T.: Ecological impacts of dams, water diversions and river management on floodplain wetlands in Australia,
421 *Austral Ecology*, 25, 109-127, <https://doi.org/10.1046/j.1442-9993.2000.01036.x>, 2000.

422 Kong, D., Latrubesse, E. M., Miao, C., and Zhou, R.: Morphological response of the Lower Yellow River to the operation of
423 Xiaolangdi Dam, China, *Geomorphology*, 350, 106931-106931, <https://doi.org/10.1016/j.geomorph.2019.106931>, 2020.

424 Kuo, C.-W., Tfwala, S., Chen, S.-C., An, H.-P., and Chu, F.-Y.: Determining transition reaches between torrents and
425 downstream rivers using a valley morphology index in a mountainous landscape, *Hydrological Processes*, 35, e14393,
426 <https://doi.org/10.1002/hyp.14393>, 2021.

427 Lai, Y. G., Greimann, B. P., and Wu, K.: Soft Bedrock Erosion Modeling with a Two-Dimensional Depth-Averaged Model,
428 *Journal of Hydraulic Engineering*, 137, 804–814, [https://doi.org/10.1061/\(asce\)hy.1943-7900.0000363](https://doi.org/10.1061/(asce)hy.1943-7900.0000363), 2011.

429 Lee, J. C., Chu, H. T., Angelier, J., Chan, Y. C., Hu, J. C., Lu, C. Y., and Rau, R. J.: Geometry and structure of northern
430 surface ruptures of the 1999 Mw = 7.6 Chi-Chi Taiwan earthquake: Influence from inherited fold belt structures, *Journal of*
431 *Structural Geology*, 24, 173-192, [https://doi.org/10.1016/S0191-8141\(01\)00056-6](https://doi.org/10.1016/S0191-8141(01)00056-6), 2002.

432 Leopold, L. B. and Wolman, M. G.: *River channel patterns: braided, meandering, and straight*, US Government Printing
433 Office, 1957.

434 Lin, A., Ouchi, T., Chen, A., and Maruyama, T.: Co-seismic displacements, folding and shortening structures along the
435 Chelungpu surface rupture zone occurred during the 1999 Chi-Chi (Taiwan) earthquake, *Tectonophysics*, 330, 225-244,
436 [https://doi.org/10.1016/S0040-1951\(00\)00230-4](https://doi.org/10.1016/S0040-1951(00)00230-4), 2001.

437 Liro, M.: Dam-induced base-level rise effects on the gravel-bed channel planform, *Catena*, 153, 143-156,
438 <https://doi.org/10.1016/j.catena.2017.02.005>, 2017.

439 Liro, M.: Dam reservoir backwater as a field-scale laboratory of human-induced changes in river biogeomorphology: A
440 review focused on gravel-bed rivers, *Science of the Total Environment*, 651, 2899-2912,
441 <https://doi.org/10.1016/j.scitotenv.2018.10.138>, 2019.

442 Lyell Sir, C., and Deshayes, G. P.: *Principles of geology; being an attempt to explain the former changes of the earth's*
443 *surface, by reference to causes now in operation*, J. Murray, London, 1830.

444 Magilligan, F. J., and Nislow, K. H.: Changes in hydrologic regime by dams, *Geomorphology*, 71, 61-78,
445 <https://doi.org/10.1016/j.geomorph.2004.08.017>, 2005.

446 Merritts, D., and Vincent, K. R.: Geomorphic response of coastal streams to low, intermediate, and high rates of uplift,
447 Medocino triple junction region, northern California, *GSA Bulletin*, 101, 1373-1388, [https://doi.org/10.1130/0016-7606\(1989\)101<1373:GROCST>2.3.CO;2](https://doi.org/10.1130/0016-7606(1989)101<1373:GROCST>2.3.CO;2), 1989.

449 Miodrag, S., and M, H. F.: 2-D Bed Evolution in Natural Watercourses—New Simulation Approach, *Journal of Waterway,*
450 *Port, Coastal, and Ocean Engineering*, 116, 425-443, [https://doi.org/10.1061/\(ASCE\)0733-950X\(1990\)116:4\(425\)](https://doi.org/10.1061/(ASCE)0733-950X(1990)116:4(425)), 1990.

451 Nelson, N. C., Erwin, S. O., and Schmidt, J. C.: Spatial and temporal patterns in channel change on the Snake River
452 downstream from Jackson Lake dam, Wyoming, *Geomorphology*, 200, 132-142,
453 <https://doi.org/10.1016/j.geomorph.2013.03.019>, 2013.

454 Olsen, N. R. B.: Two-dimensional numerical modelling of flushing processes in water reservoirs, *Journal of Hydraulic*
455 *Research*, 37, 3-16, <https://doi.org/10.1080/00221689909498529>, 1999.

456 Ota, Y., Chen, Y.-G., and Chen, W.-S.: Review of paleoseismological and active fault studies in Taiwan in the light of the
457 Chichi earthquake of September 21, 1999, *Tectonophysics*, 408, 63-77, <https://doi.org/10.1016/j.tecto.2005.05.040>, 2005.

458 Parker, G., and Izumi, N.: Purely erosional cyclic and solitary steps created by flow over a cohesive bed, *Journal of Fluid*
459 *Mechanics*, 419, 203-238, <https://doi.org/10.1017/S0022112000001403>, 2000.

460 Petts, G. E., and Gurnell, A. M.: Dams and geomorphology: research progress and future directions, *Geomorphology*, 71,
461 27-47, <https://doi.org/10.1016/j.geomorph.2004.02.015>, 2005.

462 Seidl, M. A., and Dietrich, W. E.: The problem of channel erosion into bedrock, *Functional geomorphology*, 101-124, 1992.

463 Shafroth, P. B., Perry, L. G., Rose, C. A., and Braatne, J. H.: Effects of dams and geomorphic context on riparian forests of
464 the Elwha River, Washington, *Ecosphere*, 7, e01621-e01621, <https://doi.org/10.1002/ecs2.1621>, 2016.

465 Słowik, M., Dezső, J., Marciniak, A., Tóth, G., and Kovács, J.: Evolution of river planforms downstream of dams: Effect of
466 dam construction or earlier human-induced changes?, *Earth Surface Processes and Landforms*, 43, 2045-2063,
467 <https://doi.org/10.1002/esp.4371>, 2018.

468 Surian, N., and Rinaldi, M.: Morphological response to river engineering and management in alluvial channels in Italy,
469 *Geomorphology*, 50, 307-326, [https://doi.org/10.1016/S0169-555X\(02\)00219-2](https://doi.org/10.1016/S0169-555X(02)00219-2), 2003.

470 Tomkin, J. H., Brandon, M. T., Pazzaglia, F. J., Barbour, J. R., and Willett, S. D.: Quantitative testing of bedrock incision
471 models for the Clearwater River, NW Washington State, *Journal of Geophysical Research: Solid Earth*, 108,
472 <https://doi.org/10.1029/2001jb000862>, 2003.

473 Whipple, K. X., and Tucker, G. E.: Dynamics of the stream-power river incision model: Implications for height limits of
474 mountain ranges, landscape response timescales, and research needs, *Journal of Geophysical Research: Solid Earth*, 104,
475 17661-17674, <https://doi.org/10.1029/1999jb900120>, 1999.

476 Whipple, K. X.: Fluvial landscape response time: how plausible is steady-state denudation?, *American Journal of Science*,
477 301, 313-325, <https://doi.org/10.2475/ajs.301.4-5.313>, 2001.

478 Whipple, K. X., and Tucker, G. E.: Implications of sediment-flux-dependent river incision models for landscape evolution,
479 *Journal of Geophysical Research: Solid Earth*, 107, ETG 3-1-ETG 3-20, doi.org/10.1029/2000JB000044, 2002.

480 Whipple, K. X.: BEDROCK RIVERS AND THE GEOMORPHOLOGY OF ACTIVE OROGENS, *Annual Review of Earth*
481 *and Planetary Sciences*, 32, 151-185, <https://doi.org/10.1146/annurev.earth.32.101802.120356>, 2004.

482 Williams, G. P., and Wolman, M. G.: Downstream effects of dams on alluvial rivers 1286, 1984.

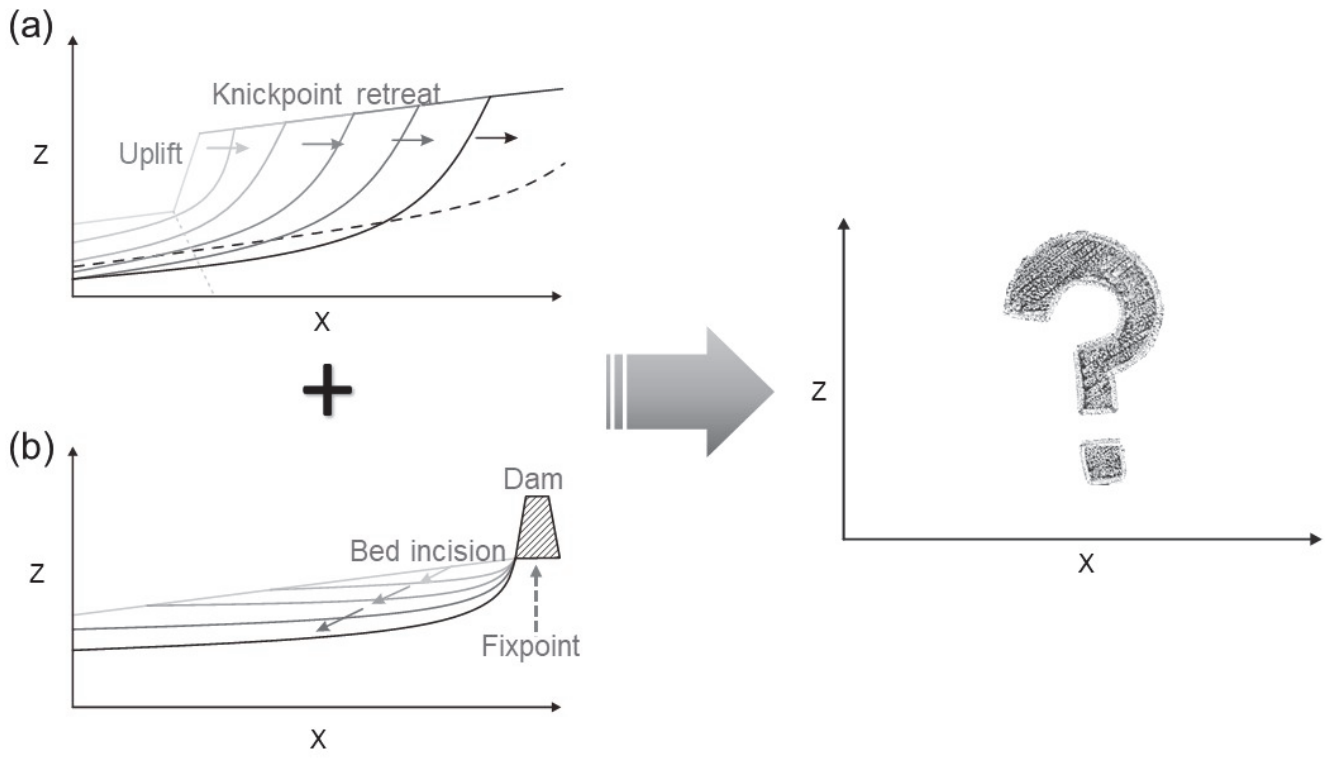
483 Zhou, M., Xia, J., Deng, S., Lu, J., and Lin, F.: Channel adjustments in a gravel-sand bed reach owing to upstream damming,
484 *Global and Planetary Change*, 170, 213-220, <https://doi.org/10.1016/j.gloplacha.2018.08.014>, 2018.

485

486

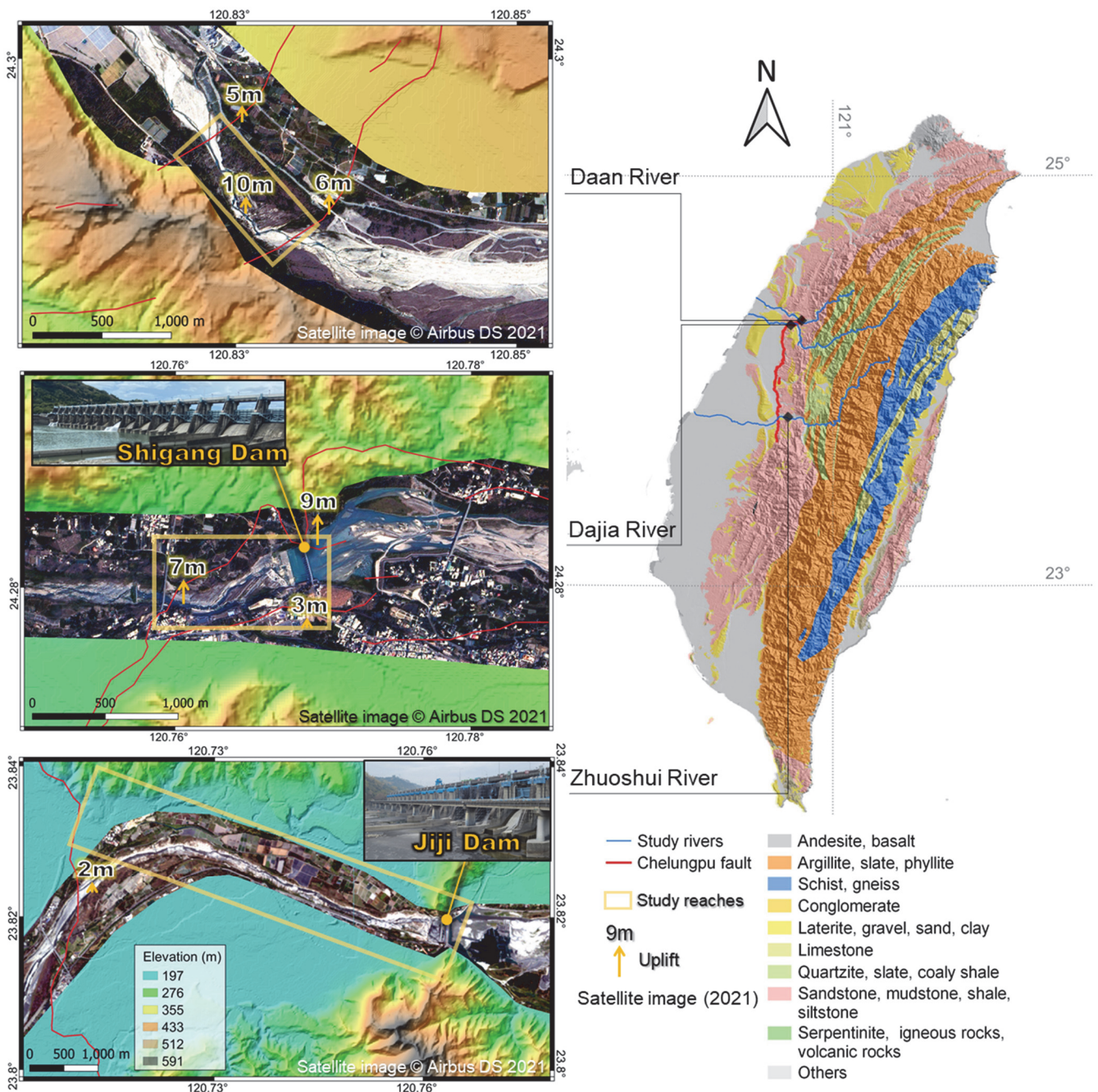
Table 1 Characteristics of the studied reaches of the Daan, Zhuoshui, and Dajia rivers

River	Time interval	Section	Bed Change		Channel Widening		Knickpoint retreat		C (m yr ⁻¹)	
			(m)	(m yr ⁻¹)	(m)	(m yr ⁻¹)	(m)	(m yr ⁻¹)		
Daan	2000–2004	a	-0.60	-0.15	-103.77	-25.94	85	21.25	22	
		b	-1.76	-0.44	47.50	11.88				
	2004–2007	a	-16.67	-5.56	-316.50	-105.50	422	140.67		
		b	-6.20	-2.07	-269.82	-89.94				
	2007–2011	a	2.06	0.52	19.30	4.83	412	103.00		
		b	-7.11	-1.78	-64.19	-16.05				
	2011–2016	a	-0.45	-0.09	31.19	6.24	--	--		
		b	-0.84	-0.17	41.27	8.25	--	--		
	Zhuoshui	1998–2008	c	-0.46	-0.05	-96.22	-9.62	--		--
			d	-2.24	-0.22	-130.41	-13.04			
e			-11.59	-1.16	-246.32	-24.63				
2008–2012		c	-5.44	-1.36	-258.44	-64.61	--	--		
		d	-2.77	-0.69	18.43	4.61				
		e	3.00	0.75	5.22	1.31				
2012–2015		c	-4.46	-1.49	-171.56	-57.19	--	--		
		d	-6.65	-2.22	-133.24	-44.41				
		e	-4.94	-1.65	-73.11	-24.37				
2015–2018		c	-0.84	-0.28	13.57	4.52	--	--		
		d	-0.86	-0.29	1.31	0.44				
		e	-3.03	-1.01	8.70	2.90				
Dajia		2000–2005	f	-2.39	-0.48	-14.12	-2.82	40	8.00	7.5
			g	-2.02	-0.40	-116.44	-23.29			
		2005–2008	f	-2.57	-0.86	-39.90	-13.30	186	62.00	
	g		-7.50	-2.50	-142.97	-47.66				
	2008–2014	f	-1.33	-0.22	12.28	2.05	219	24.33		
		g	-0.38	-0.06	2.21	0.37				
	2010–2014	h	-4.20	-1.05	-25.45	-6.36				
	2014–2017	f	-1.39	-0.46	-10.44	-3.48				
		g	-3.32	-1.11	8.84	2.95				
		h	-5.27	-1.76	-20.63	-6.88				



489

490 **Figure 1: Schematic diagrams of longitudinal profile development for (a) fault scarp's knickpoint, (b) dam's fixpoint,**
 491 **and (c) How will the combined effects develop longitudinal profile?**

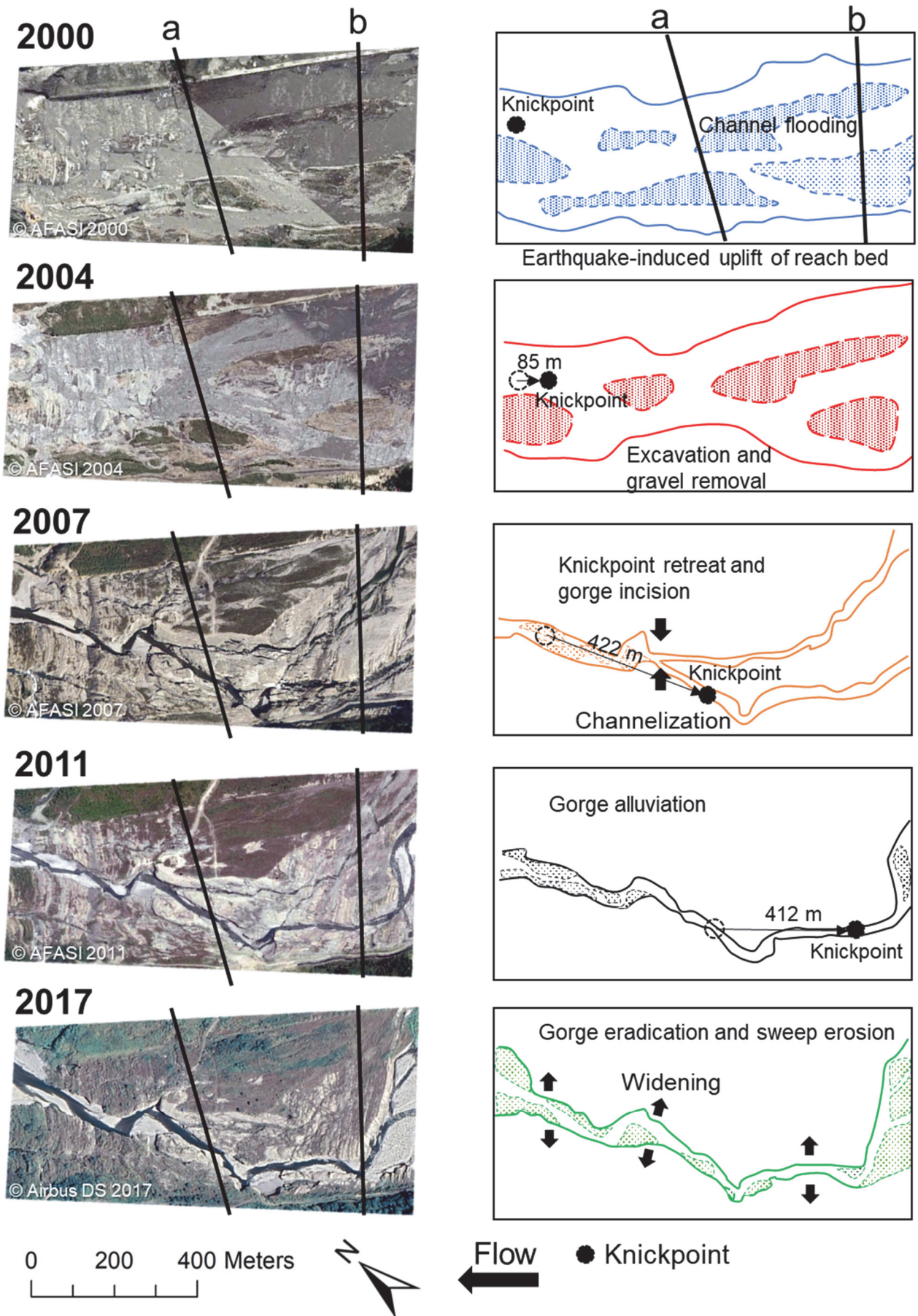


492

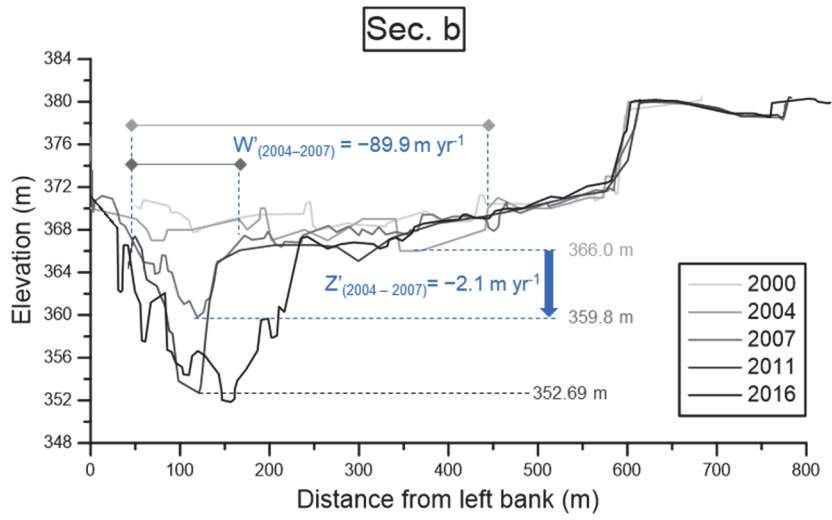
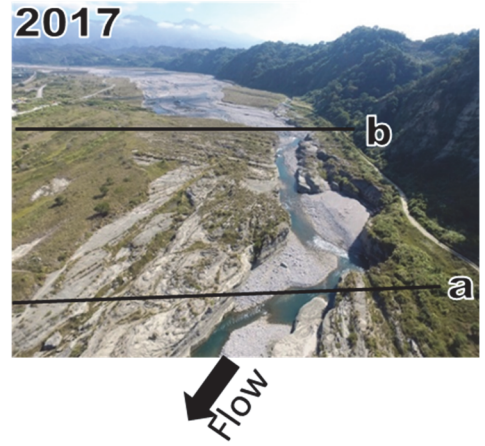
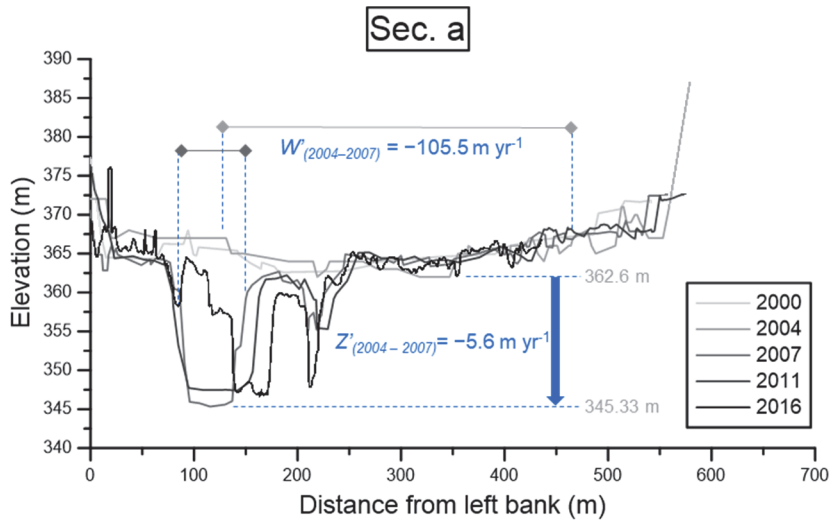
493

494

Figure 2: Locations of the Chelungpu Fault, the three studied rivers, and satellite images (from CSRSR/NCU date: 05-Feb-2021, 2m resolutions) showing the studied reaches.



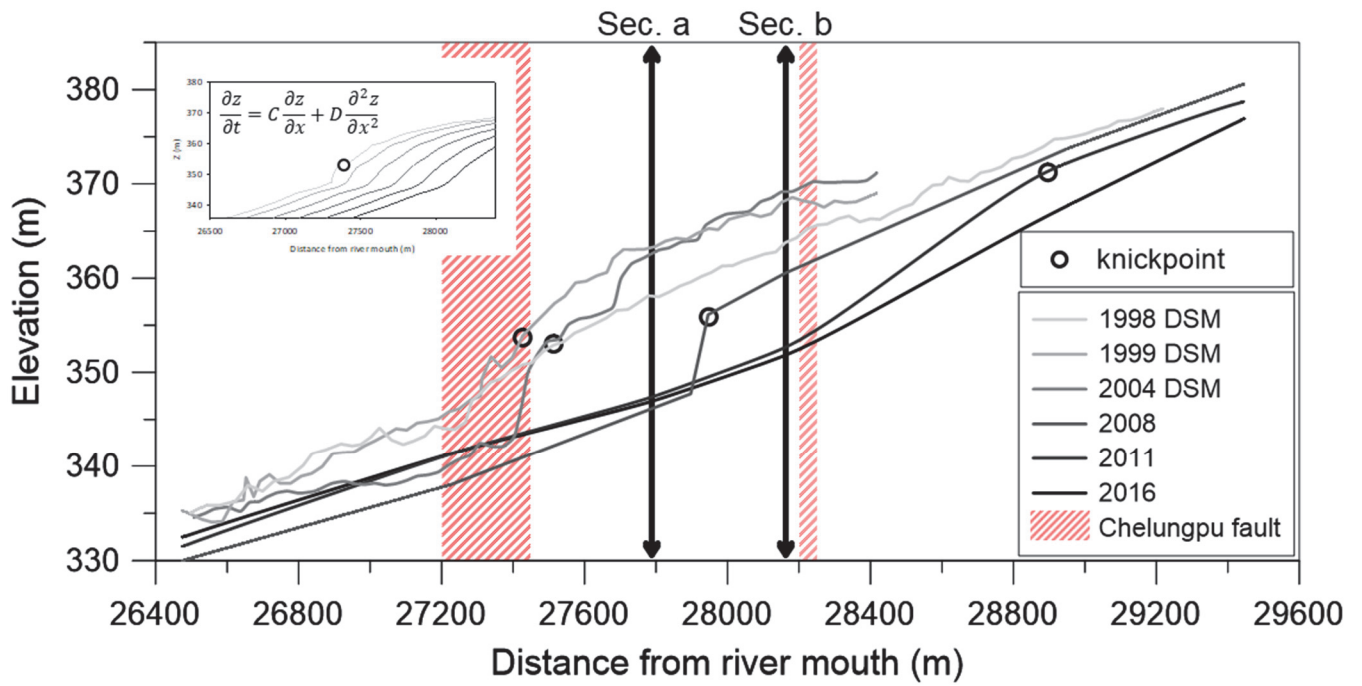
495
 496 **Figure 3: Orthographic images (2000–2011), satellite image (2017) and flow paths of the studied reach of the Daan**
 497 **River from 2000 to 2017.**



498

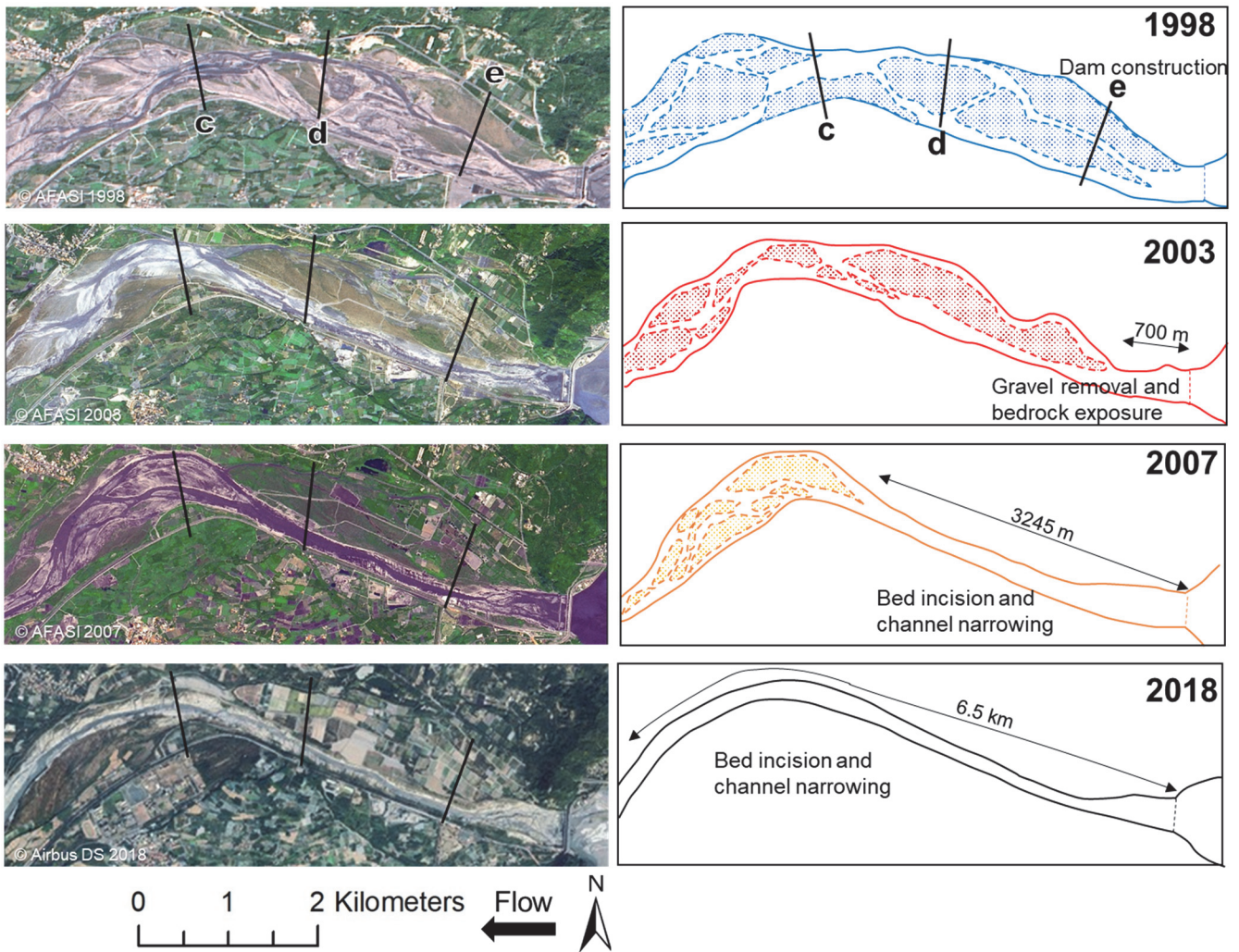
499 **Figure 4: Cross-sections a and b of the Daan River from 2000 to 2016 (from WRA).**

500



502

503 Figure 5: Longitudinal profiles of the studied reach of the Daan River from 2000 to 2016. Profiles for 1998–2008 are
 504 from Cook et al. (2013), and 2011–2016 are from WRA. Data between 1998 and 2004 are derived from aerial photograph
 505 generated Digital Surface Models (DSMs). Knickpoint retreats are simulated using the advective-diffusive model at the
 506 top left.
 507



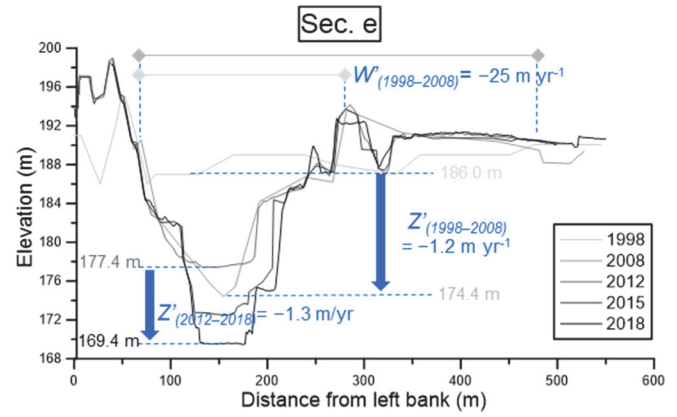
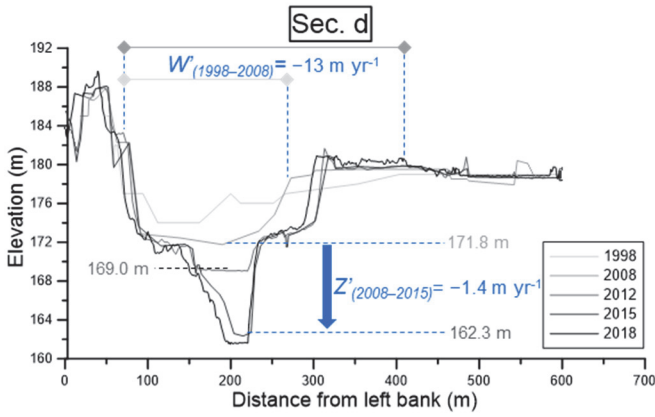
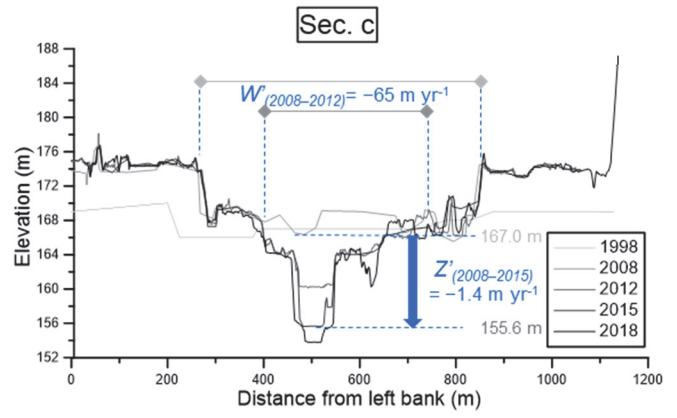
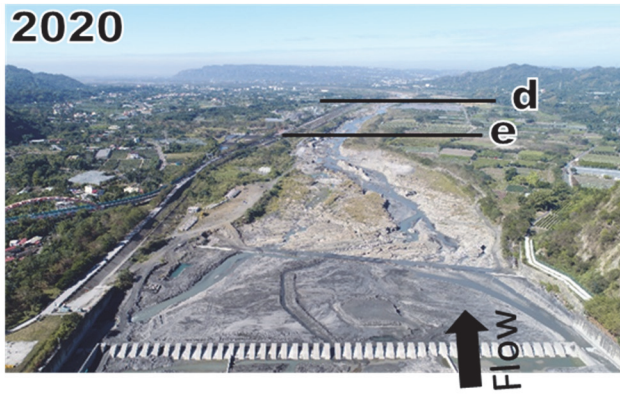
508

509

510

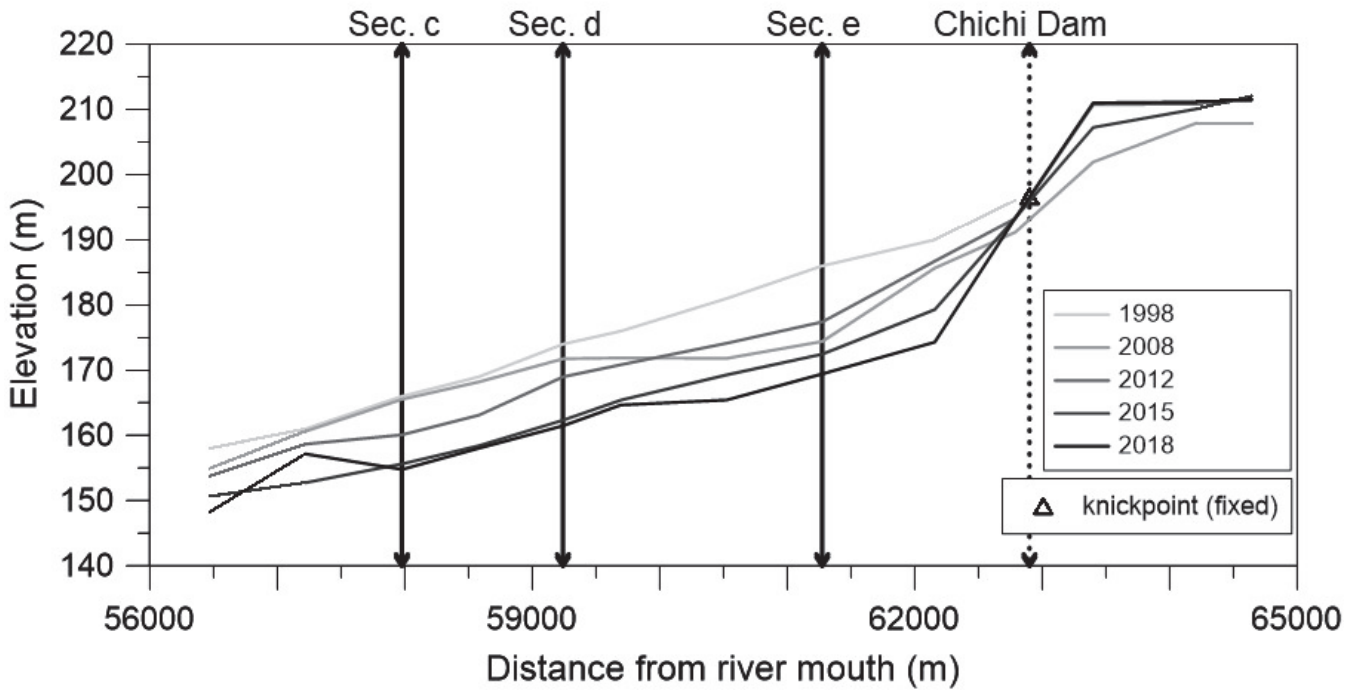
511

Figure 6: Orthographic images (1998–2007), satellite image (2018), and flow paths of the studied reach of the Zhuoshui River from 1998 to 2018.



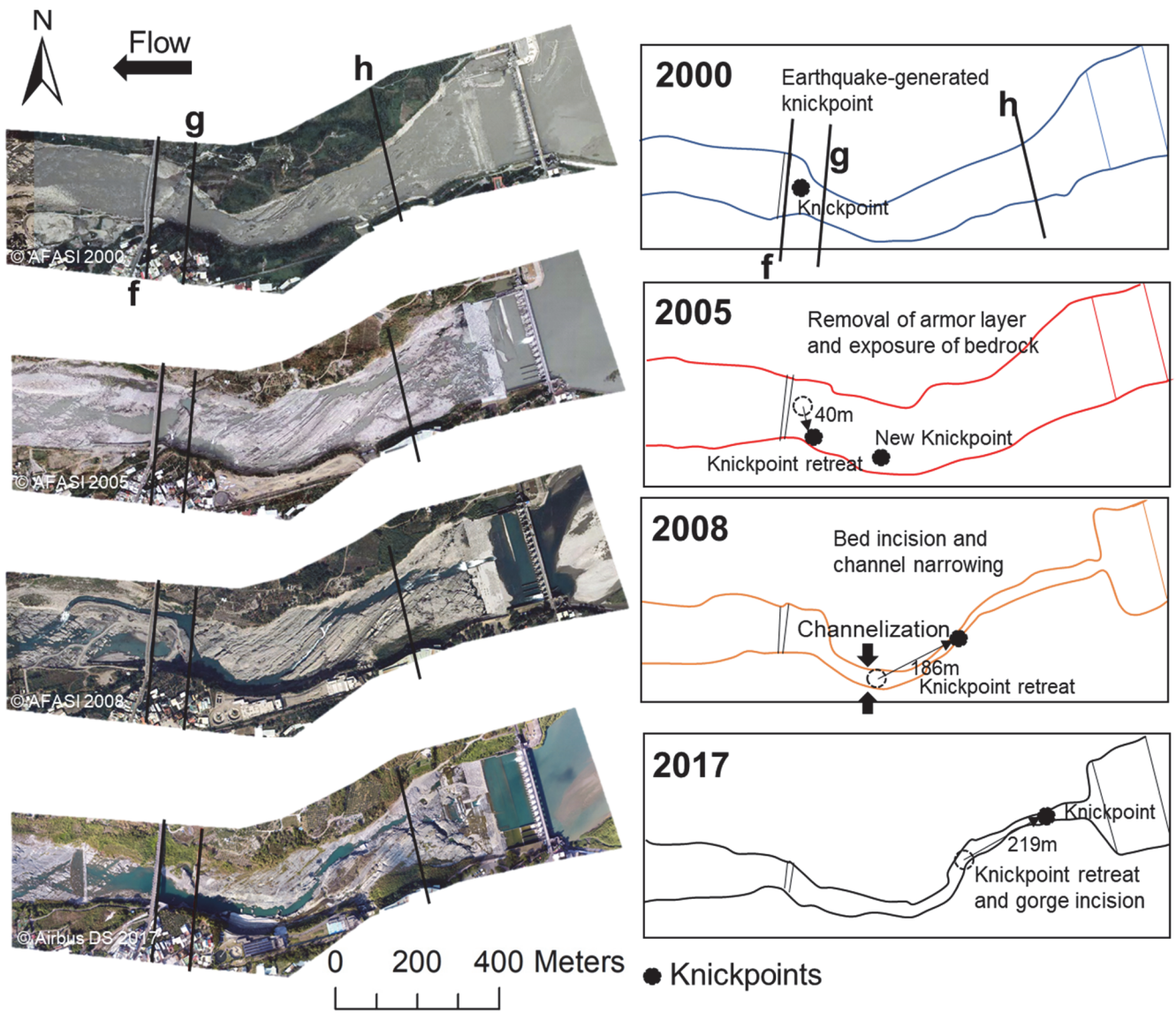
512
513

Figure 7: Profiles of cross-sections c, d, and e of the Zhuoshui River from 1998 to 2018 (from WRA).



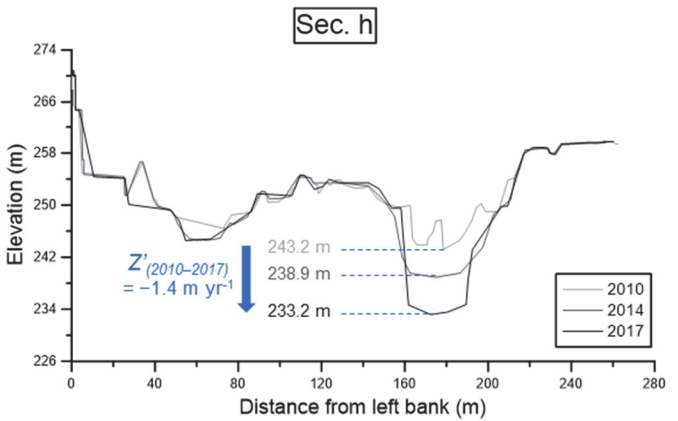
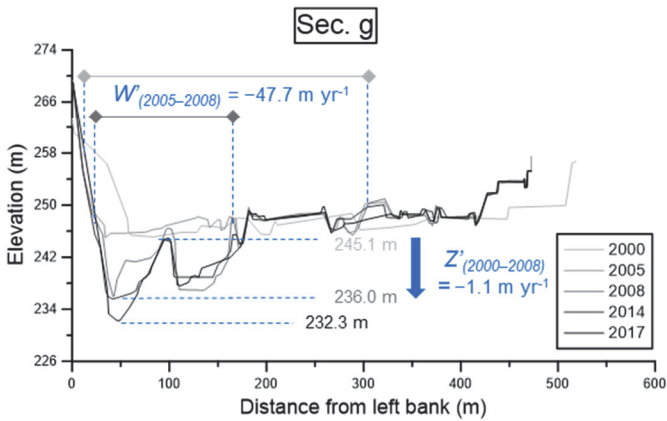
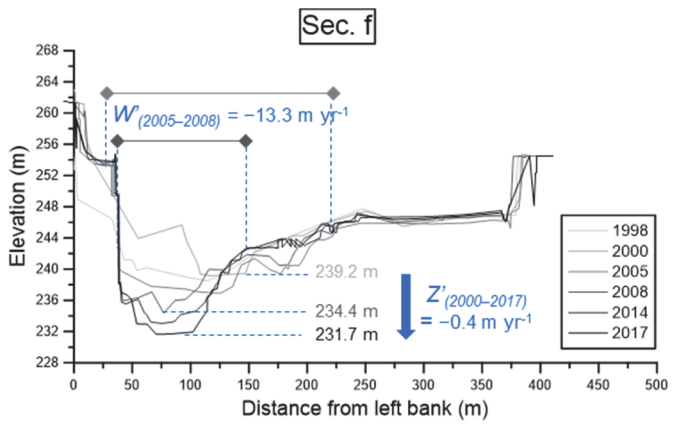
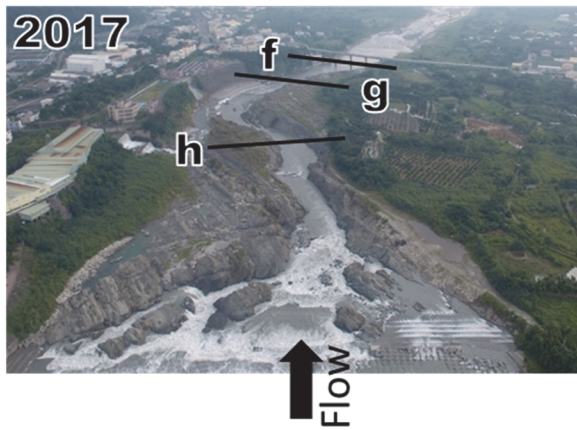
514
515

Figure 8: Longitudinal profiles of the studied reach of the Zhuoshui River from 1998 to 2018 (from WRA).



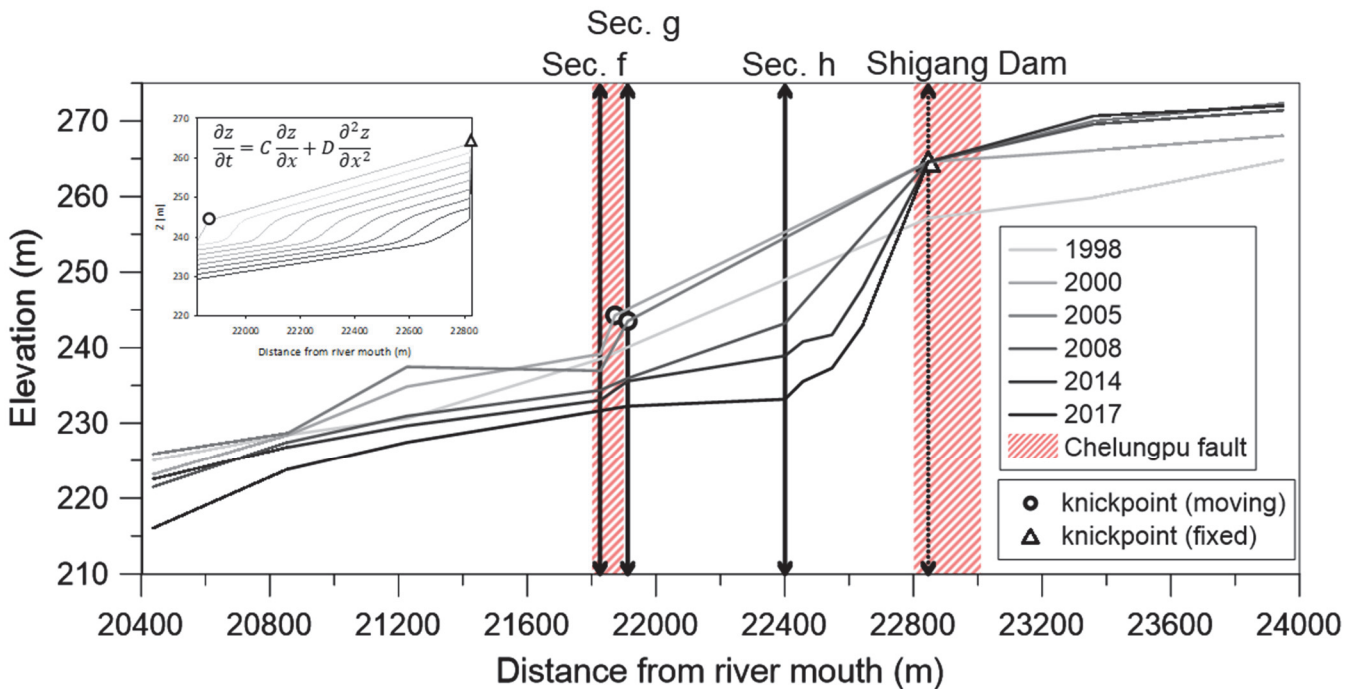
516
517
518

Figure 9: Orthographic images (2000–2008), satellite image (2017), and flow paths of the studied reach of the Dajia River from 2000 to 2017.



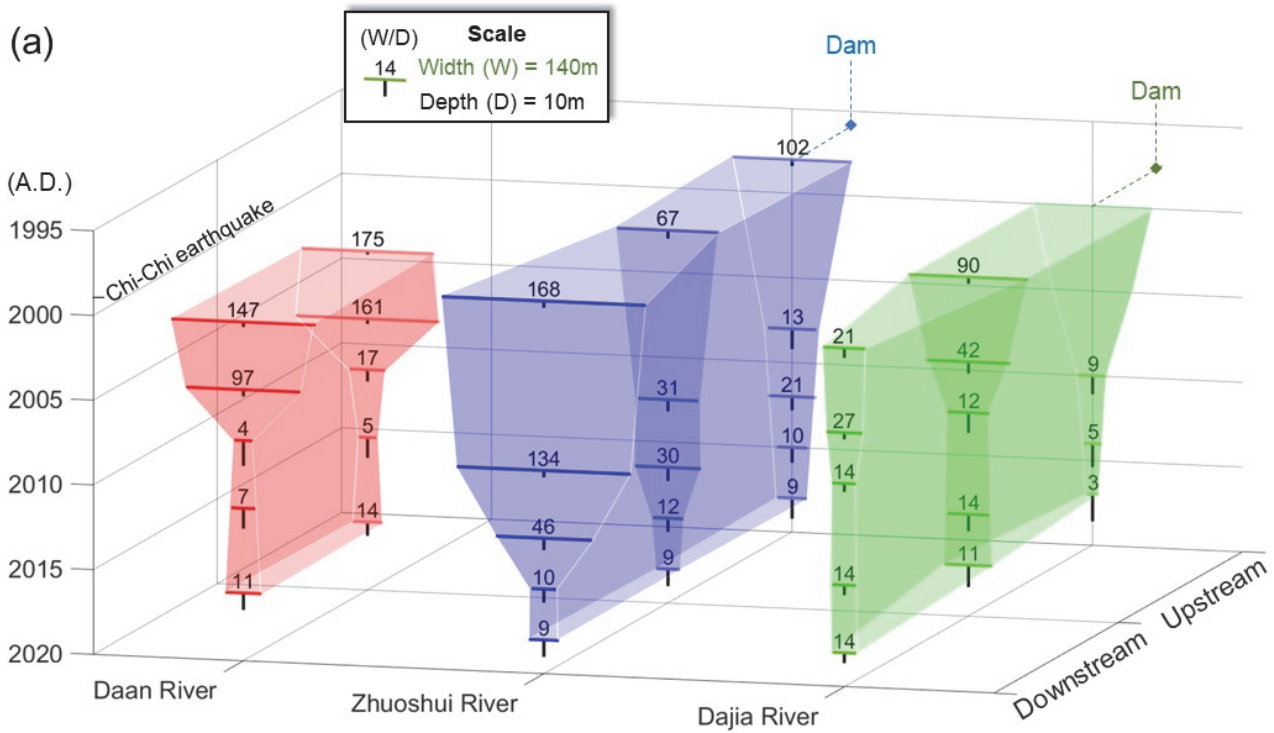
519
520

Figure 10: Cross-sections f, g, and h of the Dajia River from 2000 to 2017 (from WRA).

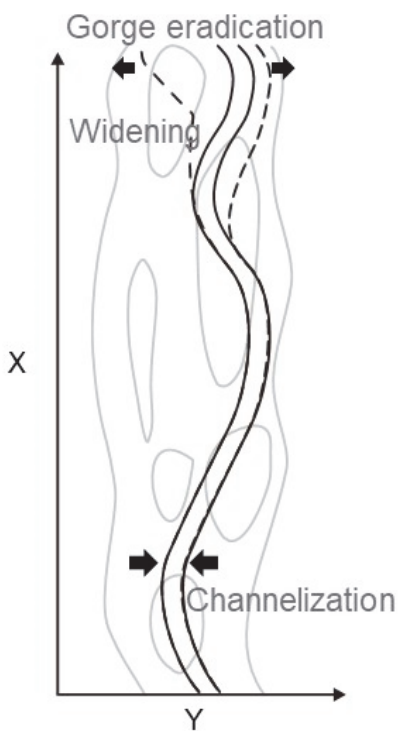


521
522
523
524

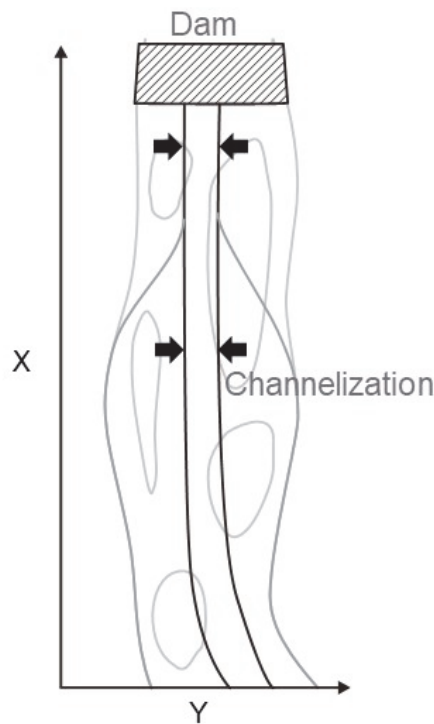
Figure 11: Longitudinal profiles of the studied reach of the Dajia River from 1998 to 2017 (from WRA). Knickpoint retreats are simulated using the advective-diffusive model at the top left.



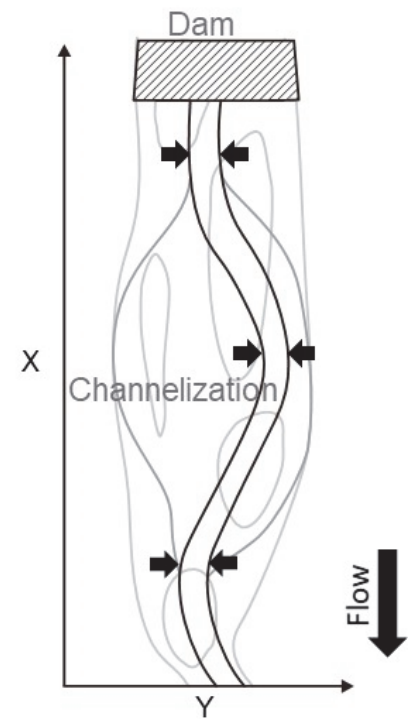
(b) Daan river



(c) Zhuoshui river



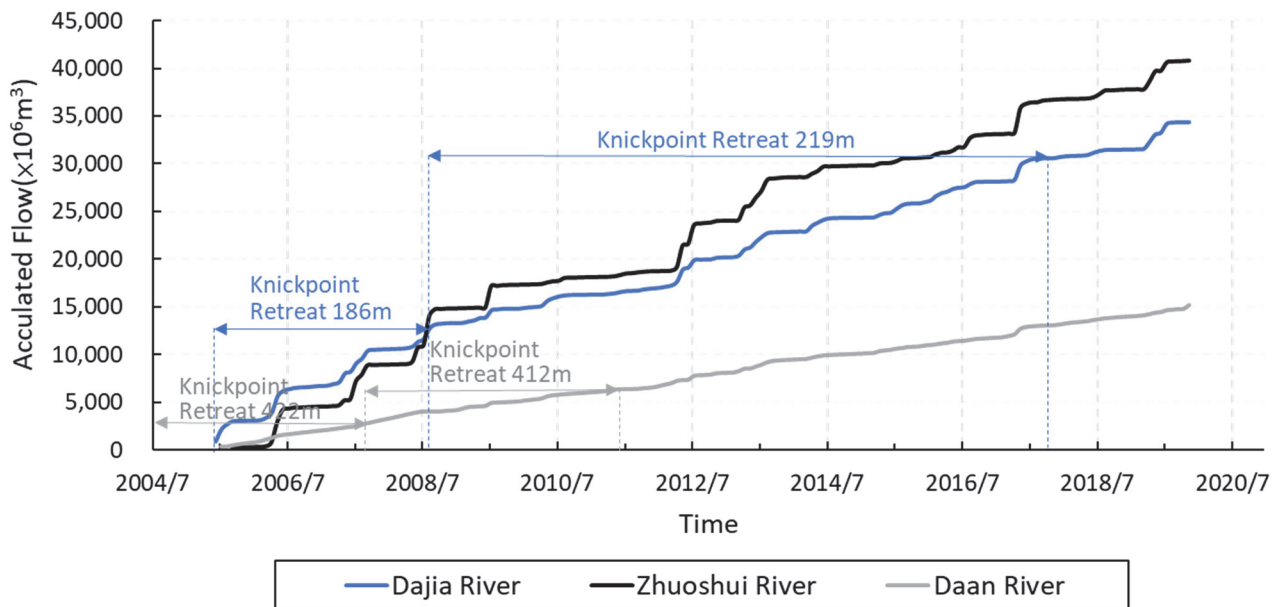
(d) Dajia river



525

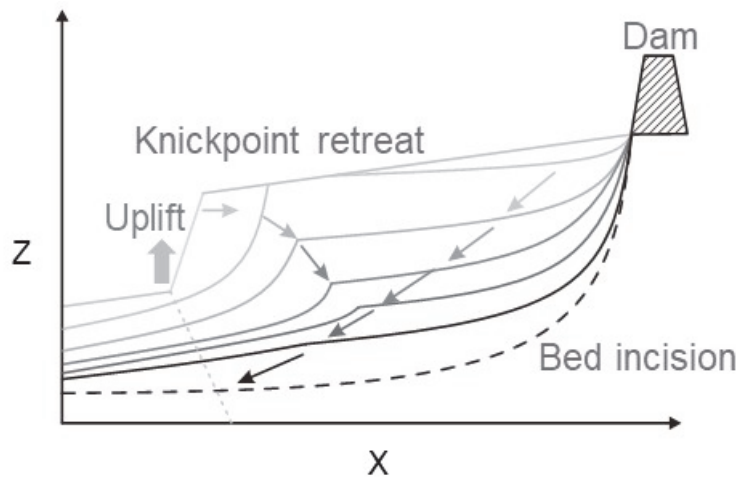
526

527 Figure 12: (a) Channel width (W), depth (D), and aspect ratio (W/D) of the studied reaches of the three rivers. The
 528 aspect ratio was defined as the ratio of the bankfull width to the depth of the bankfull channel. The vertical axis shows
 529 the time from 1995 downward to 2020, the horizontal axis shows the rivers, and the normal axis shows the sections
 530 from downstream to upstream. Schematic diagrams of knickpoint retreat and river pattern development for (b)
 531 coseismic uplift, (c) dam obstruction, and (d) dam obstruction and coseismic uplift.



532

533 Figure 13: The cumulative flow in the three study reaches and the corresponding knickpoint retreat distances.



534

535 Figure 14: A Schematic diagram of longitudinal profile development for the combined effects from dam construction
536 and coseismic uplift.

537

538